



Linear MMSE estimation of time–frequency variant channels for MIMO-OFDM systems[☆]

Pierluigi Salvo Rossi^{a,*}, Ralf R. Müller^b, Ove Edfors^c

^a Department of Information Engineering, Second University of Naples, Via Roma 29, 81031 Aversa (CE), Italy

^b Department of Electronics and Telecommunications, Norwegian University of Science and Technology, O.S. Bragstads plass 2B, 7491 Trondheim, Norway

^c Department of Electrical and Information Technology, Lund University, O. Römers väg 3, 223 63 Lund, Sweden

ARTICLE INFO

Article history:

Received 24 February 2010

Received in revised form

18 August 2010

Accepted 29 October 2010

Available online 10 November 2010

Keywords:

Channel estimation

Iterative receivers

MIMO-OFDM systems

ABSTRACT

This paper proposes two low-complexity two-dimensional channel estimators for MIMO-OFDM systems derived from a joint time–frequency channel estimator. The estimators exploit both time and frequency correlations of the wireless channel via use of Slepian-basis expansions. The computational saving comes from replacing a two-dimensional Slepian-basis expansion with two serially concatenated one-dimensional Slepian-basis expansions. Performance in terms of normalized mean square error (NMSE) vs. signal-to-noise ratio (SNR) is analyzed via numerical simulations and compared with the original estimator. The analysis of the performance takes into account the impact of both system and channel parameters. The estimators are finally tested when used within the loop of an iterative receiver for MIMO-OFDM systems.

© 2010 Elsevier B.V. All rights reserved.

1. Introduction

Design of next-generation wireless systems is focusing mainly on the use of multiple-input multiple-output (MIMO) channels [26] with orthogonal frequency-division multiplexing (OFDM) [8] providing MIMO-OFDM systems [24]. Iterative receivers [28] have shown to be very attractive from complexity-performance point of view, and have been designed [1,17,19,32] such to perform also pilot-assisted channel estimation [2]. In this paper we focus on channel estimation for MIMO-OFDM systems to be performed within the loop of an iterative receiver.

Channel estimation for OFDM systems has been proposed via singular value decomposition [4] and via discrete

Fourier transform [5] exploiting frequency correlation, and via two-dimensional Wiener filtering [9] exploiting time and frequency correlations. Robustness to channel-statistics mismatch is analyzed in [13], while complexity issues have been taken into account also via parametric channel modeling [29]. Recently, a low-complexity channel estimator for MIMO-OFDM systems has been proposed exploiting the angle-domain representation [10], in which the trade-off between performance and complexity crucially depends on the knowledge of the correlation among the various angle-frequency domain beams.

Basis expansion models [7] have shown to be very effective in dealing with time-variant channels. Exploiting the works on discrete prolate spheroidal (DPS) sequences [23], a robust low-complexity channel estimator has been proposed [31] and applied in both iterative receivers for multi-carrier code-division multiple-access systems [32] and iterative receivers for MIMO-OFDM systems [17,19]. Time and frequency variations of realistic wireless channels have been taken into account via the multidimensional DPS sequences [22,27] in the extensions proposed in [3,33] for multi-carrier code-division multiple-access systems, in [11] for MIMO systems, and in [18] for MIMO-OFDM systems.

[☆] This work has been supported by the Research Council of Norway and by the Swedish Governmental Agency for Innovation Systems under the projects WILATI and WILATI+ within the NORDITE framework. The material in this paper was presented in part at the IEEE Global Telecommunications Conference (GLOBECOM), Honolulu, HI, US, December 2009 (see [20]).

* Corresponding author.

E-mail addresses: pierluigi.salvorossi@unina2.it (P. Salvo Rossi), mueller@iet.ntnu.no (R.R. Müller), Ove.Edfors@es.lth.se (O. Edfors).

Finally, alternative approaches to channel estimation [6,21,30] are based on blind-identification techniques exploiting higher order statistics of received signals. Blind channel estimation saves spectral efficiency with respect to pilot-assisted channel estimation at the cost of less reliable estimates.

In this paper we recall the estimator proposed in [18] and propose two similar approximations, comparing their performance and complexity on the basis of channel characteristics. The benefits of the two-dimensional Slepian-based approach proposed in [18] are (i) robustness—no assumption on channel statistics is needed but knowledge of the maximum delay spread and maximum Doppler spread; (ii) low complexity—less coefficients to be estimated due to the concentration of the space; (iii) accuracy—two-dimensional processing exploits both time and frequency correlations. Such an estimator is named in the following joint channel estimator (JCE) as it performs joint time–frequency processing. In order to further reduce the computational complexity, which can still remain high for channels with large Doppler and/or delay spreads, we design two serial channel estimators (SCEs) approximating the two-dimensional time–frequency processing via serially concatenated one-dimensional processing: (i) a serial time–frequency channel estimator (STFCE) in which time processing is performed for each subcarrier and then frequency processing is applied; (ii) a serial frequency–time channel estimator (SFTCE) in which frequency processing is performed for each OFDM block and then time processing is applied.

As we here mainly focus on channel estimation, when designing and testing the channel estimators all the transmitted symbols are assumed to be known at the receiver. However, in a real iterative receiver only pilot symbols are available at the first iteration, while soft estimates from the decoder are available at successive iterations to replace (initially unknown) data symbols. Soft estimates will converge, in a well-designed receiver, to the correct values of data symbols, thus the performance of the channel estimator shown represents the maximum achievable performance. Before concluding the paper, a final test of the channel estimator will be presented by showing the performance an iterative receiver in which both transmitted symbols (excluding pilots) and channel coefficients need to be estimated. Although, we are not exploring the problem of optimal pilot placement [14,25], affecting mainly the performance of the channel estimator at the first iteration, it is worth noticing that the proposed estimators allow flexible pilot patterns. Usually, block-type (for some given time slots all subcarriers contain pilots) and comb-type (for some given subcarriers all time slots contain pilots) patterns are considered, while the proposed estimators allow, due to the two-dimensional processing, various pilot patterns that sparsely sample the time–frequency domain as long as they obey the limits of the sampling theorem set by delay spread and Doppler spread.

The contributions of this paper are mainly:

- the design of two low-complexity channel estimators that fit the same characteristics of the estimator in [18];
- the analysis of their performance with respect to the channel characteristics (such as delay and Doppler spreads) and system parameters (such as number of subcarriers and blocks in a frame);

- the verification of their performance in an iterative receiver for MIMO-OFDM systems.

The rest of the paper is organized as follows: Section 2 introduces the system model; the Slepian-basis expansion models are described in Section 3; the channel estimators are presented in Section 4; Section 5 shows the performance obtained via computer simulation in terms of normalized mean square error (NMSE) vs. signal-to-noise ratio (SNR), as well as the performance in terms of bit error rate (BER) vs. SNR of an iterative receiver for MIMO-OFDM systems employing such estimators within the loop; some concluding remarks are given in Section 6.

Notation: Column vectors (resp. matrices) are denoted with lower-case (resp. upper-case) bold letters; a_n (resp. $A_{n,m}$) denotes the n th (resp. (n,m) th) element of vector \mathbf{a} (resp. matrix \mathbf{A}); $\text{diag}(\mathbf{a})$ denotes a diagonal matrix whose main diagonal is \mathbf{a} ; \mathbf{I}_N denotes the $N \times N$ identity matrix; \mathbf{O}_N denotes the $N \times N$ null matrix; $\mathbf{i}_{N,M,L}^{(n,m,\ell)}$ denotes the $((n-1)M + m - 1)L + \ell$ th column of \mathbf{I}_{NML} ; \mathbf{e}_N denotes a vector of length N whose components are 1; \mathbf{o}_N denotes a vector of length N whose components are 0; $\mathbb{E}\{\cdot\}$, $(\cdot)^*$, $(\cdot)^T$ and $(\cdot)^H$ denote expectation, conjugate, transpose, and conjugate transpose operators; \hat{a} denotes an estimate of a ; \bar{a} denotes the expected value of a ; $\delta_{n,m}$ is the Kronecker delta; \otimes denotes the Kronecker product; $\lceil a \rceil$ denotes the smallest integer value greater than or equal to a ; j denotes the imaginary unit; $\mathcal{N}_C(\boldsymbol{\mu}, \boldsymbol{\Sigma})$ denotes a circular symmetric complex normal distribution with mean vector $\boldsymbol{\mu}$ and covariance matrix $\boldsymbol{\Sigma}$; the symbol \sim means “distributed as”.

2. Analytical model

We assume a wireless MIMO-OFDM system with K transmit antennas and N receive antennas. For data transmission, each transmit antenna uses OFDM with M subcarriers. Data are assumed to be encoded within a frame composed of S OFDM blocks, and each OFDM block is composed of M symbols. In the following, for the generic frame, $x_k[m,s]$ denotes the (*frequency domain*) symbol¹ transmitted by the k th transmit antenna on the m th subcarrier during the transmission of the s th OFDM block; $H_{n,k}[m,s]$ denotes the (*frequency domain*) channel coefficient between the k th transmit antenna and the n th receive antenna on the m th subcarrier during the transmission of the s th OFDM block; $w_n[m,s]$ denotes the (*frequency domain*) additive noise at the n th receive antenna on the m th subcarrier during the transmission of the s th OFDM block; $r_n[m,s]$ denotes the (*frequency domain*) received signal at the n th receive antenna on the m th subcarrier during the transmission of the s th OFDM block.

Optimal pilot placement falls beyond the scope of this paper. When using the STFCE we assume that pilot symbols are distributed in the frame according to a bidimensional grid in which S_p OFDM blocks present M_p pilot symbols each, thus having $L_p = M_p S_p$ pilot symbols per frame, i.e. a pilot-to-symbols ratio (PSR) equals to L_p/L , with $L = MS$ denoting the number of symbols in a single frame. More

¹ Both for pilot and data symbols.

specifically, we assume that the OFDM blocks in which pilots are present are given by the following set of indexes $\{\lceil((2s-1)S)/2S_p\rceil\}_{s=1}^{S_p}$. Also, referring to the s th OFDM block among those containing pilots, pilot symbols are distributed according to the following set of frequency indexes $\{\text{mod}(\lceil((2m-1)M)/2M_p\rceil+s-1, M)\}_{m=1}^{M_p}$, i.e. for a given OFDM block pilot symbols are placed into the subcarriers following those considered for the previous OFDM block. This choice guarantees that each subcarrier has at least one pilot symbol, thus assuring that the STFCE (explained in Section 4) may work correctly. Having at least one pilot symbol for each subcarrier is crucial in the first iteration when data symbols are unbiased (i.e. set to 0) and thus channel estimation only relies on pilot symbols.

Analogously, when using the SFTCE we assume that pilot symbols are distributed in the frame according to a bidimensional grid in which M_p subcarriers present S_p pilot symbols each, again $\text{PSR} = L_p/L$. More specifically, we assume that the subcarriers in which pilots are present are given by the following set of indexes $\{\lceil((2m-1)M)/2M_p\rceil\}_{m=1}^{M_p}$. Also, referring to the m th subcarrier among those containing pilots, pilot symbols are distributed according to the following set of time indexes $\{\text{mod}(\lceil((2s-1)S)/2S_p\rceil+m-1, S)\}_{s=1}^{S_p}$, i.e. for a given subcarrier pilot symbols are placed into the OFDM blocks following those considered for the previous subcarrier. This choice guarantees that each OFDM block has at least one pilot symbol, thus assuring that the SFTCE (explained in Section 4) may work correctly for the same reason as for STFCE.

Fig. 1 shows a frame with $M=12$ subcarriers, $S=20$ OFDM blocks, $M_p=4$ pilots along frequency and $S_p=5$ pilots along time, for both STFCE and SFTCE.

We denote the transmitted vector, the channel matrix, the noise vector, and the received vector as

$$\mathbf{x}[m,s] = (x_1[m,s], \dots, x_K[m,s])^T, \quad (1)$$

$$\mathbf{H}[m,s] = \begin{pmatrix} H_{1,1}[m,s] & \dots & H_{1,K}[m,s] \\ \vdots & \ddots & \vdots \\ H_{N,1}[m,s] & \dots & H_{N,K}[m,s] \end{pmatrix}, \quad (2)$$

$$\mathbf{w}[m,s] = (w_1[m,s], \dots, w_N[m,s])^T \sim \mathcal{N}_{\mathbb{C}}(\mathbf{0}, \sigma_w^2 \mathbf{I}_N), \quad (3)$$

$$\mathbf{r}[m,s] = (r_1[m,s], \dots, r_N[m,s])^T, \quad (4)$$

respectively, and assume that the length of the cyclic prefix (L_{cp}) exceeds the channel delay spread. Then, the discrete-time model for the received signal is

$$\mathbf{r}[m,s] = \mathbf{H}[m,s]\mathbf{x}[m,s] + \mathbf{w}[m,s]. \quad (5)$$

It is worth noticing that m and s represent frequency-variation and time-variation, respectively. The channel is considered time–frequency variant meaning that it does not remain constant within the frame: different blocks experience different correlated attenuations, and different subcarriers within the same block experience different correlated attenuations.

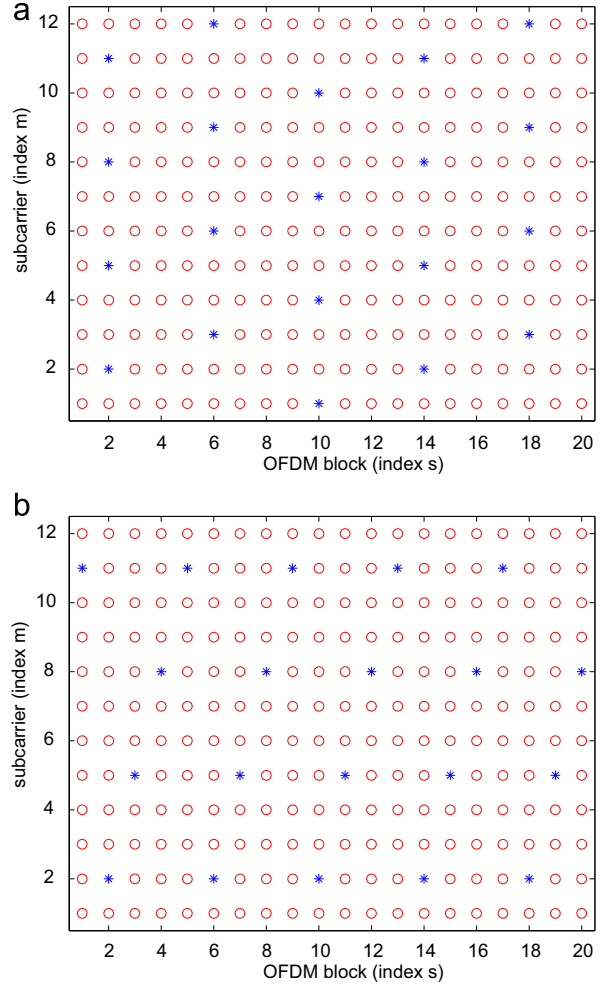


Fig. 1. Data (•) and pilot (*) symbols in a frame with $M=12$, $S=20$, $M_p=4$, $S_p=5$. Pilots placement for (a) the STFCE and (b) the SFTCE.

3. Slepian-basis expansion

We consider a wireless channel with maximum normalized delay spread $\eta_{\max}^{(d)}$ and maximum normalized Doppler spread $\nu_{\max}^{(D)}$, i.e. for each transmit/receive antennas pair, $[-\eta_{\max}^{(d)}, +\eta_{\max}^{(d)}] \times [-\nu_{\max}^{(D)}, +\nu_{\max}^{(D)}]$ is the rectangular support of the scattering function

$$\mathcal{H}_{n,k}(\eta, \nu) = \sum_{m=1}^M \sum_{s=1}^S H_{n,k}[m,s] \exp(-j2\pi(\eta m + \nu s)). \quad (6)$$

It is worth noticing that η and ν represent delay and Doppler as they correspond via a Fourier transformation to frequency index m and time index s , respectively.

Let $v_\ell[m]$ and $\lambda_\ell^{(d)}$ denote the m th sample of the ℓ th DPS sequence and the corresponding eigenvalue, for the interval $m=1, \dots, M$ and bandwidth extension $\eta_{\max}^{(d)}$; and analogously $u_i[s]$ and $\lambda_i^{(D)}$ the s th sample of the i th DPS sequence and the corresponding eigenvalue, for the interval $s=1, \dots, S$ and bandwidth extension $\nu_{\max}^{(D)}$, respectively, defined as the

solutions to

$$\sum_{m'=1}^M 2\eta_{\max}^{(d)} \text{sinc}(2\eta_{\max}^{(d)}(m'-m))v_\ell[m'] = \lambda_\ell^{(d)} v_\ell[m], \quad (7)$$

$$\sum_{s'=1}^S 2\nu_{\max}^{(D)} \text{sinc}(2\nu_{\max}^{(D)}(s'-s))u_i[s'] = \lambda_i^{(D)} u_i[s]. \quad (8)$$

The DPS sequences have resulted those bandlimited sequences simultaneously most concentrated in a finite time interval [23].

As they distinguish the two dimensions of the wireless channel,² $v_\ell[m]$ and $u_i[s]$ will be denoted frequency-DPS (f-DPS) and time-DPS (t-DPS) sequences, respectively. In [18] the following two-dimensional Slepian expansion (making use of an orthogonal basis based on DPS sequences)

$$H_{n,k}[m,s] \approx \sum_{\ell=1}^L \sum_{i=1}^I \psi_{n,k}[\ell,i] u_i[s] v_\ell[m], \quad (9)$$

has been used in order to design a channel estimator for time–frequency variant MIMO-OFDM channels, where $\psi_{n,k}[\ell,i]$ is the (ℓ,i) th “delay-Doppler Slepian coefficient” for the link between the k th transmit antenna and the n th receive antenna, $M^{(d)} \leq L \leq M$ and $S^{(D)} \leq I \leq S$, being $M^{(d)} = \lceil 2\eta_{\max}^{(d)} M \rceil + 1$ and $S^{(D)} = \lceil 2\nu_{\max}^{(D)} S \rceil + 1$ the approximate signal space extensions. The concentration of the space [23], along both delay and Doppler dimensions, is due to the eigenvalues $\lambda_\ell^{(d)}$ (resp. $\lambda_i^{(D)}$) becoming rapidly negligible for $\ell > 2\eta_{\max}^{(d)} M$ (resp. $i > 2\nu_{\max}^{(D)} S$).

In order to obtain STFCE we rearrange (9) as follows:

$$H_{n,k}[m,s] \approx \sum_{i=1}^I \varphi_{n,k}^{(D)}[m,i] u_i[s], \quad (10)$$

$$\varphi_{n,k}^{(D)}[m,i] \approx \sum_{\ell=1}^L \psi_{n,k}[\ell,i] v_\ell[m], \quad (11)$$

while in order to obtain SFTCE we rearrange (9) as follows:

$$H_{n,k}[m,s] \approx \sum_{\ell=1}^L \varphi_{n,k}^{(d)}[\ell,s] v_\ell[m], \quad (12)$$

$$\varphi_{n,k}^{(d)}[\ell,s] \approx \sum_{i=1}^I \psi_{n,k}[\ell,i] u_i[s], \quad (13)$$

where $\varphi_{n,k}^{(d)}[\ell,s]$ and $\varphi_{n,k}^{(D)}[m,i]$ are the ℓ th “delay Slepian coefficient” at the s th time slot and the i th “Doppler–Slepian coefficient” at the m th subcarrier, respectively, for the link between the k th transmit antenna and the n th receive antenna. The idea is to perform estimation along frequency and time domains separately in a concatenated way. More specifically, (10) and then (11) are used in order to perform estimation along time and then along frequency, while (12) and then (13) to perform estimation along frequency and then along time.

In the following, the vectors collecting the values of the f-DPS sequences for a given frequency and the corresponding

eigenvalues are denoted

$$\mathbf{v}[m] = (v_1[m], \dots, v_L[m])^T, \quad (14)$$

$$\boldsymbol{\lambda}^{(d)} = (\lambda_1^{(d)}, \dots, \lambda_L^{(d)})^T, \quad (15)$$

while the vectors collecting the values of the t-DPS sequences for a given time and the corresponding eigenvalues are denoted

$$\mathbf{u}[s] = (u_1[s], \dots, u_I[s])^T, \quad (16)$$

$$\boldsymbol{\lambda}^{(D)} = (\lambda_1^{(D)}, \dots, \lambda_I^{(D)})^T. \quad (17)$$

Also, we will denote

$$\mathbf{V} = (\mathbf{v}[1], \dots, \mathbf{v}[M])^T, \quad (18)$$

$$\mathbf{U} = (\mathbf{u}[1], \dots, \mathbf{u}[S])^T. \quad (19)$$

4. Channel estimation

JCE proposed in [18] was based on the following signal model for channel estimation

$$\mathbf{r} = \Xi \boldsymbol{\psi} + \mathbf{w}, \quad (20)$$

where

$$\mathbf{r}[:,s] = (\mathbf{r}^T[1,s], \dots, \mathbf{r}^T[M,s])^T, \quad (21)$$

$$\mathbf{r} = (\mathbf{r}^T[:,1], \dots, \mathbf{r}^T[:,S])^T, \quad (22)$$

where

$$\Xi[m,s] = \mathbf{I}_N \otimes (\boldsymbol{\alpha}[m,s] \otimes \mathbf{v}[m] \otimes \mathbf{u}[s])^T, \quad (23)$$

$$\Xi[:,s] = (\Xi^T[1,s], \dots, \Xi^T[M,s])^T, \quad (24)$$

$$\Xi = (\Xi^T[:,1], \dots, \Xi^T[:,S])^T, \quad (25)$$

where

$$\boldsymbol{\psi}_{n,k}[\ell, \cdot] = (\psi_{n,k}[\ell,1], \dots, \psi_{n,k}[\ell,I])^T, \quad (26)$$

$$\boldsymbol{\psi}_{n,k} = (\boldsymbol{\psi}_{n,k}^T[1, \cdot], \dots, \boldsymbol{\psi}_{n,k}^T[L, \cdot])^T, \quad (27)$$

$$\boldsymbol{\psi}_n = (\boldsymbol{\psi}_{n,1}^T, \dots, \boldsymbol{\psi}_{n,K}^T)^T, \quad (28)$$

$$\boldsymbol{\psi} = (\boldsymbol{\psi}_1^T, \dots, \boldsymbol{\psi}_N^T)^T, \quad (29)$$

and where

$$\mathbf{w}[:,s] = (\mathbf{w}^T[1,s], \dots, \mathbf{w}^T[M,s])^T, \quad (30)$$

$$\mathbf{w} = (\mathbf{w}^T[:,1], \dots, \mathbf{w}^T[:,S])^T. \quad (31)$$

JCE assumes the following expression (see [18] for details)

$$\hat{\boldsymbol{\psi}} = (\tilde{\boldsymbol{\Xi}}^H \boldsymbol{\Delta}^{-1} \tilde{\boldsymbol{\Xi}} + \mathbf{C}_\psi^{-1})^{-1} \tilde{\boldsymbol{\Xi}}^H \boldsymbol{\Delta}^{-1} \mathbf{r}, \quad (32)$$

where

$$\boldsymbol{\theta}[m,s] = \mathfrak{I}[m,s] \mathbf{e}_N, \quad (33)$$

$$\boldsymbol{\theta}[:,s] = (\boldsymbol{\theta}^T[1,s], \dots, \boldsymbol{\theta}^T[M,s])^T, \quad (34)$$

$$\boldsymbol{\Theta} = \text{diag}(\boldsymbol{\theta}[:,1])^T, \dots, \boldsymbol{\theta}[:,S])^T, \quad (35)$$

$$\boldsymbol{\Delta} = \boldsymbol{\Theta} + \sigma_w^2 \mathbf{I}_{NMS}, \quad (36)$$

² Frequency and time, or, equivalently, delay and Doppler.

$$\begin{aligned} \mathbf{C}_\psi &= \mathbb{E}\{\psi\psi^H\} \\ &= \frac{1}{2\eta_{\max}^{(d)}} \frac{1}{2v_{\max}^{(d)}} \text{diag}(\mathbf{e}_{NK} \otimes \lambda^{(d)} \otimes \lambda^{(d)}). \end{aligned} \quad (37)$$

The complexity of the estimator is dominated by the inversion of a square matrix of size NKL . As for $\tilde{\Xi} = \mathbb{E}\{\Xi\}$, it is worth noticing that an iterative receiver computes the expectation by the soft estimates from the soft-input-soft-output decoders, and also if both pilots and data symbols are known then $\Theta = \mathbf{O}_{NMS}$, while in general it accounts for the variance of the data symbols on the basis of the soft estimates available at the receiver.

4.1. STFCE

4.1.1. Time-domain expansion (exploiting Doppler dimension)

The time-domain estimator is based on (10). From (5), for a given subcarrier m , the signal model used for channel estimation in time domain is

$$\mathbf{r}[m, \cdot] = \Xi[m, \cdot] \varphi^{(D)}[m, \cdot] + \mathbf{w}[m, \cdot], \quad (38)$$

where

$$\mathbf{r}[m, \cdot] = (\mathbf{r}^T[m, 1], \dots, \mathbf{r}^T[m, S])^T, \quad (39)$$

$$\Xi[m, s] = \mathbf{I}_N \otimes (\boldsymbol{\alpha}[m, s] \otimes \mathbf{u}[s])^T, \quad (40)$$

$$\Xi[m, \cdot] = (\Xi^T[m, 1], \dots, \Xi^T[m, S])^T, \quad (41)$$

$$\varphi_{n,k}^{(D)}[m, \cdot] = (\varphi_{n,k}^{(D)}[m, 1], \dots, \varphi_{n,k}^{(D)}[m, I])^T, \quad (42)$$

$$\varphi_n^{(D)}[m, \cdot] = (\varphi_{n,1}^{(D)T}[m, \cdot], \dots, \varphi_{n,K}^{(D)T}[m, \cdot])^T, \quad (43)$$

$$\varphi^{(D)}[m, \cdot] = (\varphi_1^{(D)T}[m, \cdot], \dots, \varphi_N^{(D)T}[m, \cdot])^T, \quad (44)$$

$$\mathbf{w}[m, \cdot] = (\mathbf{w}^T[m, 1], \dots, \mathbf{w}^T[m, S])^T, \quad (45)$$

with an abuse of notation for $\Xi[m, s]$. Restricting our attention to linear channel estimators, and omitting the dependence on subcarrier (m) to simplify notation, we have the following estimator (see A.1 for details):

$$\hat{\varphi}^{(D)} = (\tilde{\Xi}^H \Delta^{-1} \tilde{\Xi} + \mathbf{C}_{\varphi^{(D)}}^{-1})^{-1} \tilde{\Xi}^H \Delta^{-1} \mathbf{r}, \quad (46)$$

where

$$\vartheta[m, s] = \sum_{k=1}^K (1 - |\tilde{\alpha}_k[m, s]|^2), \quad (47)$$

$$\boldsymbol{\vartheta}[m, \cdot] = (\vartheta[m, 1], \dots, \vartheta[m, S])^T, \quad (48)$$

$$\Theta[m, \cdot] = \text{diag}(\boldsymbol{\vartheta}[m, \cdot] \otimes \mathbf{e}_N), \quad (49)$$

$$\Delta[m, \cdot] = \Theta[m, \cdot] + \sigma_w^2 \mathbf{I}_{NS}, \quad (50)$$

$$\begin{aligned} \mathbf{C}_{\varphi^{(D)}} &= \mathbb{E}\{\varphi^{(D)}[m, \cdot] \varphi^{(D)H}[m, \cdot]\} \\ &= \frac{1}{2v_{\max}^{(d)}} \text{diag}(\mathbf{e}_{NK} \otimes \lambda^{(d)}). \end{aligned} \quad (51)$$

The complexity of the estimator is dominated by the inversion of a square matrix of size NKL . Again $\tilde{\Xi} = \mathbb{E}\{\Xi\}$ is provided by the soft-input-soft-output decoders, and if both pilots and data symbols are known then $\Theta[m, \cdot] = \mathbf{O}_{NS}$,

while in general it accounts for the variance of the data symbols on the basis of the soft estimates available at the receiver.

Also, we denote the error of the time-domain estimator

$$\boldsymbol{\varepsilon}^{(D)} = \varphi^{(D)} - \hat{\varphi}^{(D)}, \quad (52)$$

whose covariance matrix is

$$\mathbf{C}_{\boldsymbol{\varepsilon}^{(D)}} = (\tilde{\Xi}^H \Delta^{-1} \tilde{\Xi} + \mathbf{C}_{\varphi^{(D)}}^{-1})^{-1}, \quad (53)$$

as provided by the Bayesian Gauss–Markov theorem [12].

4.1.2. Frequency-domain expansion (exploiting delay dimension)

For given transmit antenna n , receive antenna k , and Doppler i , notice that

$$\varphi_{n,k}^{(D)}[m, i] = \mathbf{i}_{N,K,I}^{(n,k,i)T} \boldsymbol{\varphi}^{(D)}[m, \cdot], \quad (54)$$

$$\boldsymbol{\varepsilon}_{n,k}^{(D)}[m, i] = \mathbf{i}_{N,K,I}^{(n,k,i)T} \boldsymbol{\varepsilon}^{(D)}[m, \cdot], \quad (55)$$

thus Doppler–Slepian coefficients and errors from the time-domain estimator can be rearranged as

$$\boldsymbol{\phi}_{n,k}^{(D)}[\cdot, i] = (\varphi_{n,k}^{(D)}[1, i], \dots, \varphi_{n,k}^{(D)}[M, i])^T, \quad (56)$$

$$\mathbf{q}_{n,k}^{(D)}[\cdot, i] = (\boldsymbol{\varepsilon}_{n,k}^{(D)}[1, i], \dots, \boldsymbol{\varepsilon}_{n,k}^{(D)}[M, i])^T, \quad (57)$$

where defining

$$\sigma_{(n,k,i)}^{(D)2}[m, \cdot] = \mathbf{i}_{N,K,I}^{(n,k,i)T} \mathbf{C}_{\boldsymbol{\varepsilon}^{(D)}}[m, \cdot] \mathbf{i}_{N,K,I}^{(n,k,i)}, \quad (58)$$

the covariance matrix for the errors results

$$\mathbf{C}_{\boldsymbol{\phi}^{(D)}}^{(n,k,i)} = \text{diag}(\sigma_{(n,k,i)}^{(D)2}[1, \cdot], \dots, \sigma_{(n,k,i)}^{(D)2}[M, \cdot]). \quad (59)$$

From (11) and (52), the signal model used for channel estimation in frequency domain is

$$\hat{\boldsymbol{\phi}}_{n,k}^{(D)}[\cdot, i] = \mathbf{V} \boldsymbol{\psi}_{n,k}[\cdot, i] + \mathbf{q}_{n,k}^{(D)}[\cdot, i]. \quad (60)$$

Restricting our attention to linear channel estimators, and omitting the dependence on receive antenna (n), transmit antenna (k), and Doppler component (i) to simplify notation, we have the following estimator (see Section A.2 for details)

$$\hat{\boldsymbol{\psi}} = (\mathbf{V}^H \mathbf{C}_{\boldsymbol{\phi}^{(D)}}^{-1} \mathbf{V} + \mathbf{C}_{\boldsymbol{\psi}}^{-1})^{-1} \mathbf{V}^H \mathbf{C}_{\boldsymbol{\phi}^{(D)}}^{-1} \hat{\boldsymbol{\phi}}^{(D)}, \quad (61)$$

where

$$\begin{aligned} \mathbf{C}_{\boldsymbol{\psi}_{n,k}[\cdot, i]} &= \mathbb{E}\{\boldsymbol{\psi}_{n,k}[\cdot, i] \boldsymbol{\psi}_{n,k}^H[\cdot, i]\} \\ &= \frac{\lambda_i^{(d)}}{2v_{\max}^{(d)} 2\eta_{\max}^{(d)}} \text{diag}(\lambda^{(d)}). \end{aligned} \quad (62)$$

The complexity of the estimator is dominated by the inversion of a square matrix of size L .

4.2. SFTCE

Reversing the role of frequency and time domains, and equivalently of delay and Doppler dimensions, we can have an analogous dual estimator. The first step is based on a frequency-domain expansion, exploiting delay dimension via (12), and provides an estimator whose complexity is dominated by the inversion of a square matrix of size NKL .

The second step is based on a time-domain expansion, exploiting Doppler dimension via (13), and provides an estimator whose complexity is dominated by the inversion of a square matrix of size I .

4.3. One-dimensional estimators

As reference terms, in order to show the gain provided by time–frequency processing, the performance of two one-dimensional channel estimators will be also considered in Section 5. The first one is a time channel estimator (TCE) that applies Eq. (46) independently for each subcarrier, thus exploiting only the time correlation of the channel. It is the estimator considered in the receiver analyzed in [17]. The second one is an analogous dual frequency channel estimator (FCE) working independently for each block, thus exploiting only the frequency correlation of the channel.

4.4. Complexity

The complexity of each estimator is mainly due to two contributions: (i) “data preparation”, dominated by the Kronecker products for the signal model when computing the matrices Ξ , \mathbf{A} , and \mathbf{C} ; (ii) “coefficient computation”, dominated by the matrix inversion for LMMSE estimation. As for the first contribution we assume that the complexity of a Kronecker product between two vectors of size M and N , respectively, is $\mathcal{O}(MN)$. As for the second contribution we assume that the complexity for the inversion of a square matrix of size N is $\mathcal{O}(N^3)$, although there exist algorithms with lower complexity based on QR decomposition.

As for the complexity of JCE, the first contribution comes from preparing (32), while the second contribution is related to one single application of (32); thus we simply consider

$$C_{\text{JCE}}^{(I)} \approx N^2 KMSLI + NMS + (NK)^2 LI, \quad (63)$$

$$C_{\text{JCE}}^{(II)} \approx (NKLI)^3. \quad (64)$$

As for the complexity of STFCE, the first contribution comes from preparing (46), while the second contribution is related to M applications (one per subcarrier) of (46), and then NKI applications (one per combination of receive antenna, transmit antenna, and Doppler component) of (61); thus we simply consider

$$C_{\text{STF}}^{(I)} \approx N^2 KMI + NMS + (NK)^2 I, \quad (65)$$

$$C_{\text{STF}}^{(II)} \approx M(NKI)^3 + (NKI)L^3. \quad (66)$$

As for the complexity of SFTCE we have

$$C_{\text{SFT}}^{(I)} \approx N^2 KSL + NMS + (NK)^2 L, \quad (67)$$

$$C_{\text{SFT}}^{(II)} \approx S(NKL)^3 + (NKL)I^3, \quad (68)$$

obtained as the dual case of the complexity of STFCE.

Assuming for the reduced space extensions the following approximations $L = 2\eta_{\max}^{(d)} M$ and $I = 2v_{\max}^{(D)} S$, we have the expressions provided by Tables 1 and 2 for the first and the second contributions, respectively, to the complexity.

Table 1

First contribution to the complexity of the estimators.

JCE	$(NMS)(NK(2\eta_{\max}^{(d)}S)(2v_{\max}^{(D)}M) + NK^2(2\eta_{\max}^{(d)})(2v_{\max}^{(D)})) + 1$
STFCE	$(NS)(NK(2v_{\max}^{(D)}M) + NK^2(2v_{\max}^{(D)})) + M$
SFTCE	$(NM)(NK(2\eta_{\max}^{(d)}S) + NK^2(2\eta_{\max}^{(d)})) + S$

Table 2

Second contribution to the complexity of the estimators.

JCE	$(4\eta_{\max}^{(d)}v_{\max}^{(D)})^3(NKMS)^3$
STFCE	$M(2v_{\max}^{(D)})^3(NKS)^3 + (2v_{\max}^{(D)})(2\eta_{\max}^{(d)})^3(NKS)M^3$
SFTCE	$S(2\eta_{\max}^{(d)})^3(NKM)^3 + (2\eta_{\max}^{(d)})(2v_{\max}^{(D)})^3(NKM)S^3$

It is apparent how for very small spreads SCE has greater complexity than JCE, rapidly moving to opposite behavior with increasing spreads. Approximately, for symmetric scenarios ($N=K$, $M=S=g$, $\eta_{\max}^{(d)} = v_{\max}^{(D)} = \zeta$), defining $\rho_1 = (2\zeta)g^2$ and $\rho_2 = (2\zeta)^3g^2$, then the first contribution (resp. the second contribution) of SCE's saves computational complexity with respect to the first contribution (resp. the second contribution) of JCE if the following condition holds

$$\rho_1 > 1 \quad (\text{resp. } \rho_2 > 1), \quad (69)$$

the larger ρ_1 and ρ_2 , the more saving in computation (see Appendix B). Analogous conditions may be found for asymmetric scenarios.

Fig. 2 compares the performance of JCE and both SCE's for systems with 2×2 up to 16×16 antennas, with frames of size 64×64 on channels with normalized spreads (0.01,0.01), (0.03,0.03), (0.05,0.05).

5. Simulation results

Performance of the various channel estimators is evaluated and compared by means of NMSE, computed via numerical simulations as follows:

$$\delta_H = \frac{\mathbb{E}\{|H_{n,k}[m,s] - \hat{H}_{n,k}[m,s]|^2\}}{\mathbb{E}\{|H_{n,k}[m,s]|^2\}}.$$

Two typologies of channels are considered, namely: (i) “square channel”, presenting a rectangular support in the delay–Doppler domain; (ii) “V-stripe channel”, presenting two parallel vertical segments as support in the delay–Doppler domain,³ i.e. stressing the U–shape statistics of the popular Jakes model for Rayleigh fading [16].

The effects of various combinations of delay spread, Doppler spread, number of subcarriers, and number of OFDM blocks, have been analyzed on the channel estimators presented in Section 4, for both square and V-stripe channels. Systems with $K=2$ transmit antennas and $N=2$ receive antennas have been considered. The reference scenario has the following parameters: $M=64$ subcarriers, $S=64$ OFDM blocks, normalized delay spread $\eta_{\max}^{(d)} = 0.05$, normalized Doppler spread $v_{\max}^{(D)} = 0.05$. BPSK modulation

³ This has been obtained filtering out small-Doppler components.

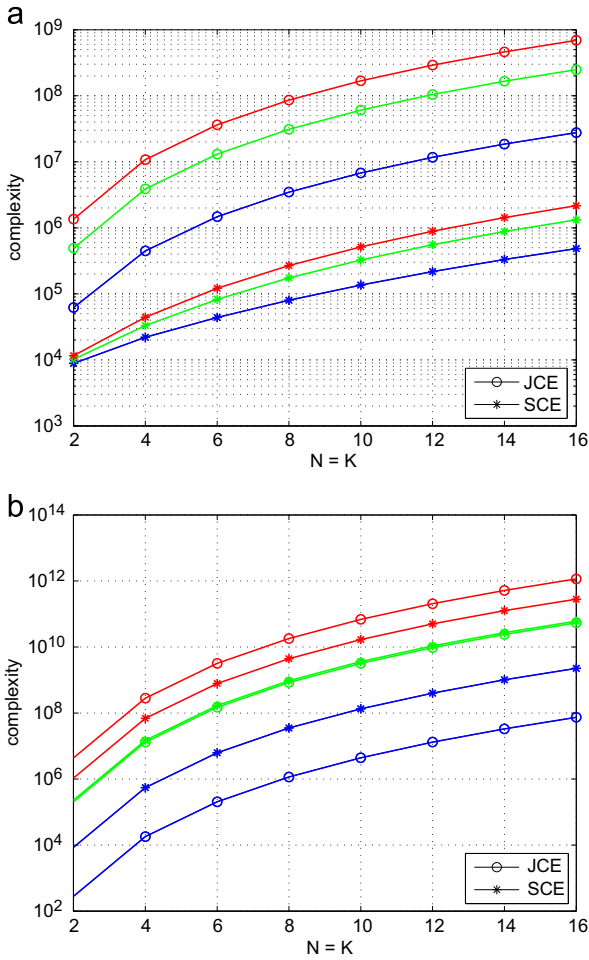


Fig. 2. Computational complexity of JCE and SCE, for $M=S=64$, in the following cases: $\eta_{\max}^{(d)} = \nu_{\max}^{(D)} = 0.01$ in blue, $\eta_{\max}^{(d)} = \nu_{\max}^{(D)} = 0.03$ in green, $\eta_{\max}^{(d)} = \nu_{\max}^{(D)} = 0.05$ in red. (a) First contribution. (b) Second contribution. (For interpretation of the references to color in this figure legend, the reader is referred to the web version of this article.)

is considered, and all transmitted symbols are assumed known at the receiver, thus resembling the best achievable performance of an iterative receiver, in which data symbols are replaced with soft estimates fed back from the decoders.

Fig. 3 shows the effects of increasing both the delay spread and the Doppler spread, simultaneously. Parameters are kept as for the reference scenario, with exception of $\eta_{\max}^{(d)}$ and $\nu_{\max}^{(D)}$ being increased with the constraint of being equal. Obviously, performance get worse with increasing delay and Doppler spreads. However, it is interesting noticing how in the square channel case both SCEs behave the same and very close to the JCE, while in the V-stripe channel case, the SFTCE is close to the JCE but the STFCE is some dB away from it. The reason is that for most of the Doppler range there is only noise contribution, thus starting with time-domain expansion is not effective. For the same reason FCE behaves even better for high SNR. Similarly, not shown here for brevity, H-stripe channels (horizontal segments) show a dual behavior with STFCE

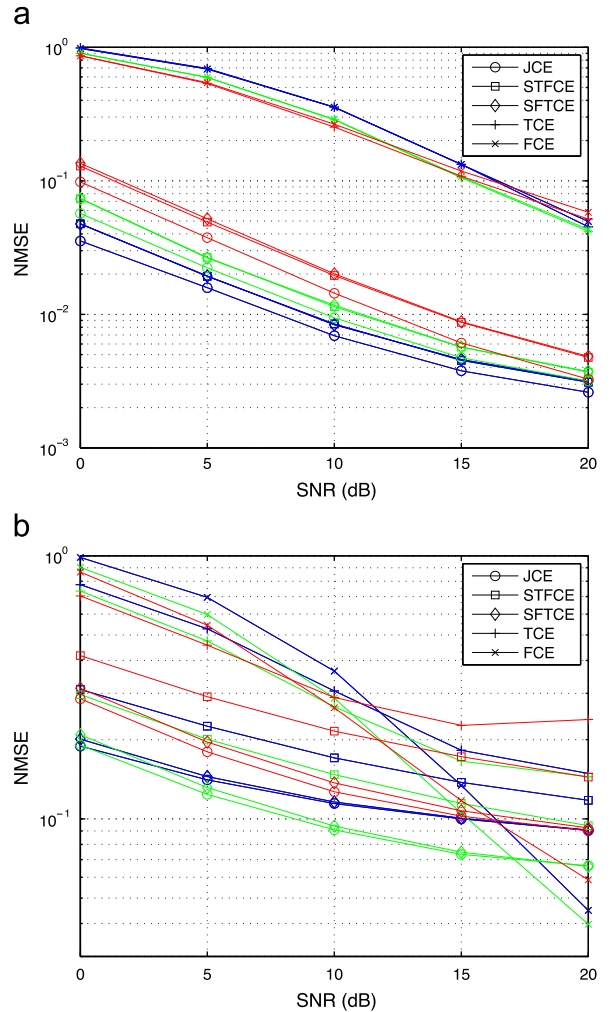


Fig. 3. Increasing $\eta_{\max}^{(d)} = \nu_{\max}^{(D)}$. Performance of the channel estimators for $N=K=2$ and $M=S=64$, in the following cases: (i) $\eta_{\max}^{(d)} = \nu_{\max}^{(D)} = 0.05$ in blue; (ii) $\eta_{\max}^{(d)} = \nu_{\max}^{(D)} = 0.07$ in green; (iii) $\eta_{\max}^{(d)} = \nu_{\max}^{(D)} = 0.1$ in red. (a) Square channel. (b) V-stripe channel. (For interpretation of the references to color in this figure legend, the reader is referred to the web version of this article.)

close to JCE, SFTCE some dB away, and TCE well performing at high SNR.

The effect of the delay spread has been analyzed keeping the parameters as for the reference scenario with exception of $\eta_{\max}^{(d)}$ being increased. Analogously the effect of the number of subcarriers has been analyzed keeping the parameters as for the reference scenario with exception of M being increased. Also, we have considered the case in which both $\eta_{\max}^{(d)}$ and M are increased while the remaining parameters are kept as for the reference scenario. The main effect is separating performance of SFTCE from JCE. FCE results better than TCE for low SNR, and vice versa for high SNR. For brevity, the effects of increasing both the delay spread and the number of subcarriers are shown in Fig. 4. Parameters are kept as for the reference scenario, with exception of $\eta_{\max}^{(d)}$ and M being increased. It is apparent the gap in performance between SFTCE and JCE. Similarly, not shown here for brevity, increasing the Doppler spread

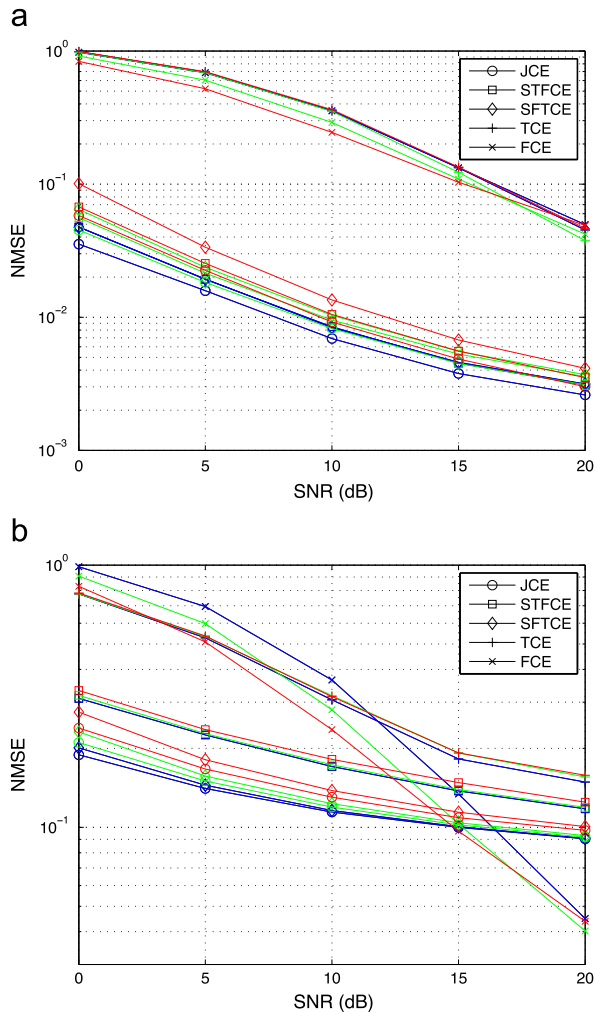


Fig. 4. Increasing $\eta_{\max}^{(d)}$ and M . Performance of the channel estimators for $N=K=2$, $S=64$ and $v_{\max}^{(D)}=0.05$, in the following cases: (i) $M=64$, $\eta_{\max}^{(d)}=0.05$ in blue; (ii) $M=80$, $\eta_{\max}^{(d)}=0.07$ in green; (iii) $M=96$, $\eta_{\max}^{(d)}=0.1$ in red. (a) Square channel. (b) V-stripe channel. (For interpretation of the references to color in this figure legend, the reader is referred to the web version of this article.)

and/or the number of OFDM blocks has the dual effect of separating performance of STFCE from JCE.

Fig. 5 shows the effects of increasing both the delay spread and the number of OFDM blocks. Parameters are kept as for the reference scenario, with exception of $\eta_{\max}^{(d)}$ and S being increased. The main effect is separating performance of SFTCE from JCE at low SNR, and both SCES at high SNR with STFCE keeping better than SFTCE. FCE results better than TCE for low SNR, and vice versa for medium and high SNR. Similarly, not shown here for brevity, increasing both the Doppler spread and the number of subcarriers has the dual effect of separating performance of STFCE and SFTCE from JCE, with SFTCE keeping better than STFCE.

Summarizing what happens in ideal conditions, i.e. when all transmitted data are available at the receiver, we can say that: (i) $\eta_{\max}^{(d)} > v_{\max}^{(D)}$ (quite reasonable in most scenario) makes STFCE perform better than SFTCE;

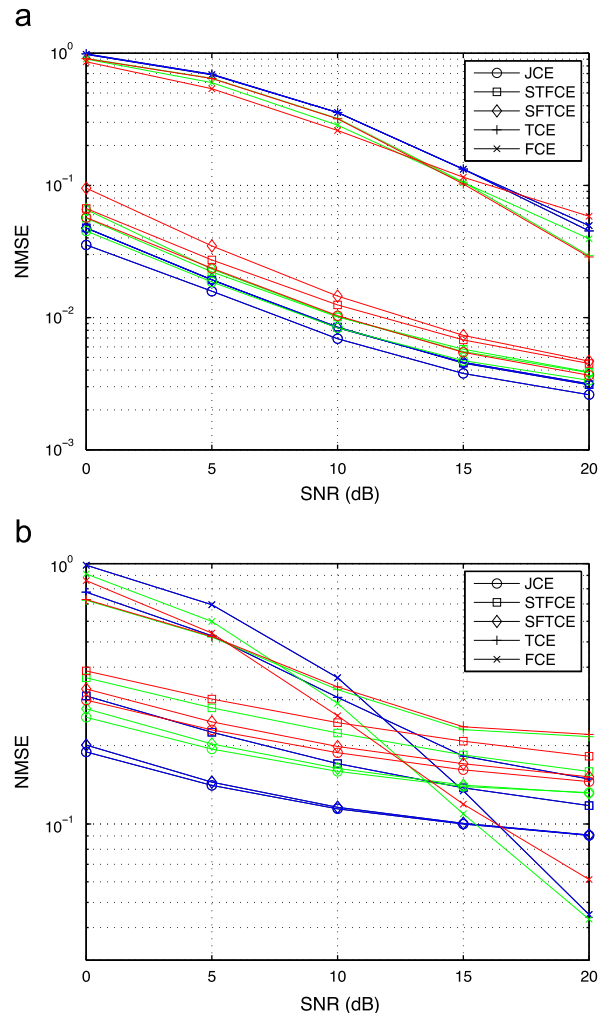


Fig. 5. Increasing $\eta_{\max}^{(d)}$ and S . Performance of the channel estimators for $N=K=2$, $M=64$ and $v_{\max}^{(D)}=0.05$, in the following cases: (i) $S=64$, $\eta_{\max}^{(d)}=0.05$ in blue; (ii) $S=80$, $\eta_{\max}^{(d)}=0.07$ in green; (iii) $S=96$, $\eta_{\max}^{(d)}=0.1$ in red. (a) Square channel. (b) V-stripe channel. (For interpretation of the references to color in this figure legend, the reader is referred to the web version of this article.)

(ii) $M > S$ (reasonable for delay-sensitive applications) makes STFCE perform better than SFTCE; (iii) channel statistics following a Jakes model for Rayleigh fading (very common assumption) make SFTCE perform better than STFCE. It is worth noticing also that SFTCE is to be preferred for delay-sensitive applications, as at each discrete time a new OFDM block is available and frequency-domain estimation (first step) can be run, while STFCE needs to wait for reception of the whole frame before running time-domain estimation (first step).

Fig. 6 shows the performance of the proposed estimators when inserted within the loop of an iterative receiver for MIMO-OFDM systems (for more details, see [17,19]). Simulations refer to a system with $K=2$ transmit antennas, $N=2$ receive antennas, $M=64$ subcarriers per OFDM block, $S=64$ OFDM blocks per frame, $M_p=24$ and $S_p=16$ corresponding to a PSR of less than 10% (similar results have

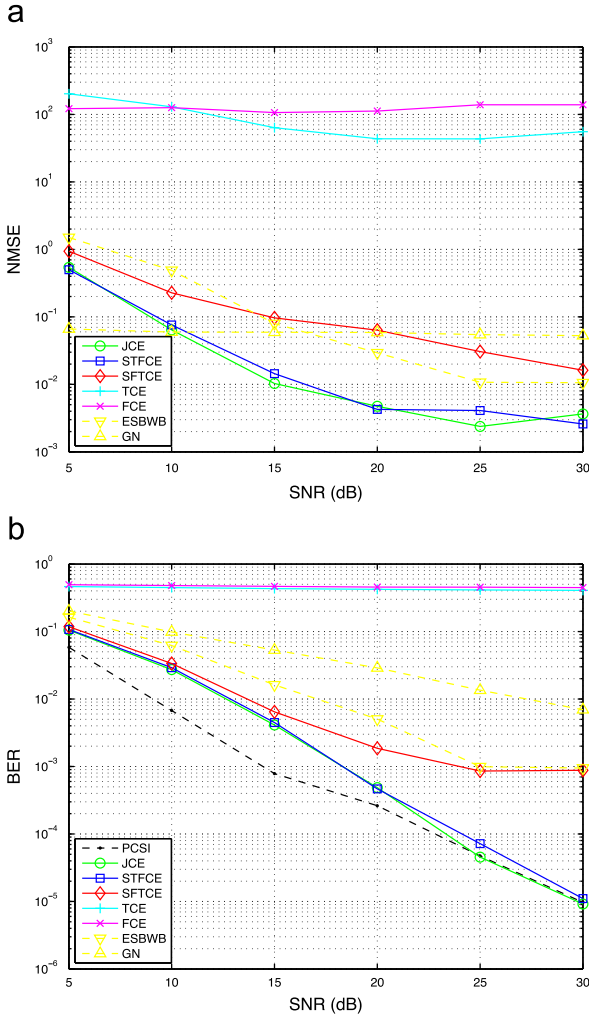


Fig. 6. Performance of an iterative receiver (at fifth iteration) for MIMO-OFDM systems with $N=K=2$, $M=S=64$, $M_p=24$, $S_p=16$ over a wireless channel with $\eta_{\max}^{(d)}=0.01$ and $v_{\max}^{(D)}=0.001$. (a) NMSE vs. SNR. (b) BER vs. SNR.

been obtained in the range 5–15%). Excluding pilots, each frame contains 3840 QPSK symbols encoding 3838 information bits via a rate-1/2 recursive systematic convolutional code with generators $(7, 5)_8$ and two tail bits to enforce the final state [15]. Channel coefficients have been generated with Rayleigh fading statistics according to a Jakes model [34] with $\eta_{\max}^{(d)}=0.01$ and $v_{\max}^{(D)}=0.001$. In a system operating at 2 GHz with OFDM block duration of 4 μ s, such parameters correspond to a scenario with maximum velocity of 135 km/h and maximum delay of 2.56 μ s, i.e. suited for urban environments and vehicular speeds.

The number of iteration at the receiver is set to 5 and the performance of a system with Perfect Channel State Information (PCSI) are shown as a reference term. Also, for comparison purpose, the performance of analogous systems using two different channel estimators (denoted with the initials of the last names of the proposing researchers) are shown. The first one, namely ESBWB, is

based on [4,5] for channel coefficients corresponding to OFDM block transmitting pilot symbols and then on linear interpolation in frequency domain in order to recover the whole set of channel coefficients. The second one, namely GN, is based on the first method proposed in [6], with $p=1/2$ and pilot symbols transmission in order to resolve the matrix ambiguity. The number of OFDM blocks for pilots transmission in both ESBWB and GN has been chosen in order to have the same PSR of the proposed systems, i.e. $M_p=64$ and $S_p=6$. It is apparent how TCE and FCE are unable to operate in such a scenario, while two-dimensional processing is necessary to approach PCSI performance. It is also apparent how STFCE performance is very close to JCE performance, while unfortunately, SFTCE saturates at relatively large SNR. Both ESBWB and GN exhibit relatively bad performance in the considered scenario as they are not able to deal effectively with the time-varying nature of the channel. More specifically, GN as well as others blind channel estimators require a large number of OFDM symbols to process in order to build reliable statistics of the received signals. Finally, to have an idea of the processing time for the joint and serial approaches, the estimation of one single channel realization, using MATLAB (R2007a) on a MacBook Pro, took on average 9.2×10^{-2} and 2.1×10^{-4} s, respectively.

6. Conclusion

Two low-complexity two-dimensional channel estimators for MIMO-OFDM systems have been designed in order to exploit in a serial way both time and frequency correlations of the wireless channel via use of a Slepian expansion. Their complexity and their performance have been compared to an analogous two-dimensional channel estimator performing joint processing of time and frequency correlations. Performance in terms of NMSE vs. SNR has been analyzed for the case in which both pilots and data are available at the receiver, corresponding to the maximum performance achievable by an iterative receiver. Computer simulations have shown how the proposed serial estimators achieve comparable performance with the joint estimator, although presenting a much lower computational complexity. The choice of the system parameters and the shape of the delay-Doppler scattering function of the wireless channels have impact on the achieved performance. Finally, the estimators have been tested with excellent results within the loop of an iterative receiver for MIMO-OFDM systems.

Appendix A. LMMSE estimation for STFCE

A.1. Time-domain LMMSE estimator

In order to simplify notation, we omit the dependence on subcarrier (m). Denote

$$\boldsymbol{\varphi}^{(D)} = \mathbf{A}^{(D)} \mathbf{r}, \quad (\text{A.1})$$

$$\mathcal{J}^{(D)}(\mathbf{A}) = \mathbb{E}\{|\boldsymbol{\varphi}^{(D)} - \mathbf{A}\mathbf{r}|^2\}, \quad (\text{A.2})$$

the linear estimate for the Doppler–Slepian coefficients and the considered cost function, respectively. The estimator is

found as

$$\mathbf{A}^{(D)} = \underset{\mathbf{A}}{\operatorname{argmin}}(\mathcal{J}^{(D)}(\mathbf{A})), \quad (\text{A.3})$$

i.e. null of

$$\nabla_{\mathbf{A}}(\mathcal{J}^{(D)}(\mathbf{A})) = 2\mathbb{E}\{\mathbf{r}\mathbf{r}^H\}\mathbf{A}^H - 2\mathbb{E}\{\mathbf{r}\boldsymbol{\varphi}^{(D)H}\}, \quad (\text{A.4})$$

thus

$$\mathbf{A}^{(D)} = \mathbb{E}\{\boldsymbol{\varphi}^{(D)}\mathbf{r}^H\}(\mathbb{E}\{\mathbf{r}\mathbf{r}^H\})^{-1}. \quad (\text{A.5})$$

From (38)

$$\begin{aligned} \mathbb{E}\{\mathbf{r}\mathbf{r}^H\} &= \mathbb{E}\{(\Xi\boldsymbol{\varphi}^{(D)} + \mathbf{w})(\Xi\boldsymbol{\varphi}^{(D)} + \mathbf{w})^H\} \\ &= \mathbb{E}\{\Xi\mathbf{C}_{\varphi^{(D)}}\Xi^H\} + \sigma_w^2\mathbf{I}_{NS}, \end{aligned} \quad (\text{A.6})$$

$$\begin{aligned} \mathbb{E}\{\boldsymbol{\varphi}^{(D)}\mathbf{r}^H\} &= \mathbb{E}\{\boldsymbol{\varphi}^{(D)}(\Xi\boldsymbol{\varphi}^{(D)} + \mathbf{w})^H\} \\ &= \mathbf{C}_{\varphi^{(D)}}\tilde{\Xi}^H. \end{aligned} \quad (\text{A.7})$$

The diagonal structure of $\mathbf{C}_{\varphi^{(D)}}$ is due to the independence of channels among different transmit antennas and/or receive antennas, and to the orthogonality of the DPS sequences

$$\mathbb{E}\{\varphi_{n,k}^{(D)}[m,i]\varphi_{n',k'}^{(D)*}[m,i']\} = \frac{\lambda_i^{(D)}}{2v_{\max}^{(D)}}\delta_{n,n'}\delta_{k,k'}\delta_{i,i'}. \quad (\text{A.8})$$

The independence of transmit antennas, and due to the effect of random interleaving, also of OFDM blocks, gives

$$\mathbb{E}\{x_k[m,s]x_{k'}^*[m,s']\} = \begin{cases} 1 & k = k', s = s', \\ \tilde{x}_k[m,s]\tilde{x}_{k'}^*[m,s'] & \text{else.} \end{cases} \quad (\text{A.9})$$

Some algebra allows to show that

$$\mathbb{E}\{\Xi\mathbf{C}_{\varphi^{(D)}}\Xi^H\} = \tilde{\Xi}\mathbf{C}_{\varphi^{(D)}}\tilde{\Xi}^H + \boldsymbol{\Theta}. \quad (\text{A.10})$$

Substitution of (A.6), (A.7) and (A.10) into (A.5) gives the estimator

$$\mathbf{A}^{(D)} = \mathbf{C}_{\varphi^{(D)}}\tilde{\Xi}^H(\tilde{\Xi}\mathbf{C}_{\varphi^{(D)}}\tilde{\Xi}^H + \boldsymbol{\Delta})^{-1}. \quad (\text{A.11})$$

Matrix inversion lemma gives (46) replacing the inversion of an $NS \times NS$ matrix with the inversion of an $NKI \times NKI$ matrix, saving computations when $K < 1/(2v_{\max}^{(D)})$. Also, both $\mathbf{C}_{\varphi^{(D)}}$ and $\boldsymbol{\Delta}$ are diagonal, thus their inversion is not computationally prohibitive.

A.2. Frequency-domain LMMSE estimator

In order to simplify notation, we omit the dependence on receive antenna (n), transmit antenna (k), and Doppler component (i). Denote

$$\hat{\boldsymbol{\psi}} = \mathbf{B}^{(d)}\boldsymbol{\phi}^{(D)}, \quad (\text{A.12})$$

$$\mathcal{J}^{(d)}(\mathbf{B}) = \mathbb{E}\{|\boldsymbol{\psi} - \mathbf{B}\boldsymbol{\phi}^{(D)}|^2\}, \quad (\text{A.13})$$

the linear estimate for the delay & Doppler–Slepian coefficients and the considered cost function. The estimator is found as

$$\mathbf{B}^{(d)} = \underset{\mathbf{B}}{\operatorname{argmin}}(\mathcal{J}^{(d)}(\mathbf{B})), \quad (\text{A.14})$$

i.e. null of

$$\nabla_{\mathbf{B}}(\mathcal{J}^{(d)}(\mathbf{B})) = 2\mathbb{E}\{\boldsymbol{\phi}^{(D)}\boldsymbol{\phi}^{(D)H}\}\mathbf{B}^H - 2\mathbb{E}\{\boldsymbol{\phi}^{(D)}\boldsymbol{\psi}^H\}, \quad (\text{A.15})$$

thus

$$\mathbf{B}^{(d)} = \mathbb{E}\{\boldsymbol{\psi}\boldsymbol{\phi}^{(D)H}\}(\mathbb{E}\{\boldsymbol{\phi}^{(D)}\boldsymbol{\phi}^{(D)H}\})^{-1}. \quad (\text{A.16})$$

From (60)

$$\begin{aligned} \mathbb{E}\{\boldsymbol{\phi}^{(D)}\boldsymbol{\phi}^{(D)H}\} &= \mathbb{E}\{(\mathbf{V}\boldsymbol{\psi} + \mathbf{q}^{(D)})(\mathbf{V}\boldsymbol{\psi} + \mathbf{q}^{(D)})^H\} \\ &= \mathbf{V}\mathbf{C}_{\psi}\mathbf{V}^H + \mathbf{C}_{q^{(D)}}, \end{aligned} \quad (\text{A.17})$$

$$\begin{aligned} \mathbb{E}\{\boldsymbol{\psi}\boldsymbol{\phi}^{(D)H}\} &= \mathbb{E}\{\boldsymbol{\psi}(\mathbf{V}\boldsymbol{\psi} + \mathbf{q}^{(D)})^H\} \\ &= \mathbf{C}_{\psi}\mathbf{V}^H. \end{aligned} \quad (\text{A.18})$$

Substitution of (A.17) and (A.18) into (A.16) gives the estimator

$$\mathbf{B}^{(d)} = \mathbf{C}_{\psi}\mathbf{V}^H(\mathbf{V}\mathbf{C}_{\psi}\mathbf{V}^H + \mathbf{C}_{q^{(D)}})^{-1}. \quad (\text{A.19})$$

Matrix inversion lemma gives (61) replacing the inversion of an $M \times M$ matrix with the inversion of an $L \times L$ matrix, saving computations for $\eta_{\max}^{(d)} < 1/2$. Also, both \mathbf{C}_{ψ} and $\mathbf{C}_{q^{(D)}}$ are diagonal, thus their inversion is not computationally prohibitive.

Appendix B. Comparison of the computational complexity

Assuming a symmetric scenario ($a=N=K$, $g=M=S$, and $\zeta = \eta_{\max}^{(d)} = v_{\max}^{(D)}$), then from Table 1 we have for the first contribution

$$C_J^{(I)} = C_{\text{JCE}} = ag^2((2\zeta)^2(ag)^2 + (2\zeta)^2a^3 + 1),$$

$$C_S^{(I)} = C_{\text{STFCE}} = C_{\text{SFTCE}} = ag((2\zeta)a^2g + (2\zeta)a^3 + g),$$

while from Table 2 we have for the second contribution

$$C_J^{(II)} = C_{\text{JCE}} = (2\zeta)^6(ag)^6,$$

$$C_S^{(II)} = C_{\text{STFCE}} = C_{\text{SFTCE}} = (2\zeta)^3(a^2g^4)(a^4 + 2\zeta).$$

Then

$$\frac{C_J^{(I)}}{C_S^{(I)}} \approx \rho_1, \quad \frac{C_J^{(II)}}{C_S^{(II)}} \approx \rho_2,$$

where the approximation holds when

$$2\zeta > \frac{1}{a^2},$$

also noticing that

$$\frac{(2\zeta)^2a^3}{(2\zeta)^2(ag)^2} < \frac{\max(a)}{\min(g)^2} \ll 1,$$

$$\frac{(2\zeta)a^3}{(2\zeta)a^2g} < \frac{\max(a)}{\min(g)} \ll 1,$$

$$\frac{2\zeta}{a^4} < \frac{2\max(\zeta)}{\min(a)^4} = \frac{1}{16} \ll 1.$$

References

- [1] J. Akhtman, L. Hanzo, Iterative receiver architectures for MIMO-OFDM, in: Proceedings of IEEE Wireless Communications and Networking Conference (WCNC), March 2007, pp. 825–829.

- [2] S. Coleri, M. Ergen, A. Puri, A. Bahai, Channel estimation techniques based on pilot arrangement in OFDM systems, *IEEE Trans. Broadcast.* 48 (3) (2002) 223–229.
- [3] C. Dumard, T. Zemen, Low-complexity MIMO multiuser receiver: a joint antenna detection scheme for time-varying channels, *IEEE Trans. Signal Process.* 56 (7) (2008) 2931–2940.
- [4] O. Edfors, M. Sandell, J.J. van de Beek, S.K. Wilson, P.O. Börjesson, OFDM channel estimation by singular value decomposition, *IEEE Trans. Commun.* 46 (7) (1998) 931–939.
- [5] O. Edfors, M. Sandell, J.J. van de Beek, S.K. Wilson, P.O. Börjesson, Analysis of DFT-based channel estimators for OFDM, *KAP Wireless Pers. Commun.* 12 (1) (2000) 55–70.
- [6] F. Gao, A. Nallanathan, Blind channel estimation for MIMO OFDM systems via nonredundant linear precoding, *IEEE Trans. Signal Process.* 55 (2) (2007) 784–789.
- [7] G.B. Giannakis, C. Telepedinlioglu, Basis expansion models and diversity techniques for blind identification and equalization of time-varying channels, *Proc. IEEE* 86 (10) (1998) 1969–1986.
- [8] A. Goldsmith, *Wireless Communications*, Cambridge University Press, 2005.
- [9] P. Hoeher, S. Kaiser, P. Robertson, Two-dimensional pilot-symbol-aided channel estimation by wiener filtering, in: *Proceedings of IEEE International Conference on Acoustics, Speech, and Signal Processing (ICASSP)*, April 1997, pp. 1845–1848.
- [10] L. Huang, J.W.M. Bergmans, F.M.J. Willems, Low-complexity LMMSE-based MIMO-OFDM channel estimation via angle-domain processing, *IEEE Trans. Signal Process.* 55 (12) (2007) 5668–5681.
- [11] F. Kaltenberger, T. Zemen, C.W. Ueberhuber, Low-complexity geometry-based MIMO channel simulation, *EURASIP J. Adv. Signal Process.* 2007 (2007) 17pp, article ID 95281.
- [12] S.M. Kay, *Fundamentals of Statistical Signal Processing: Estimation Theory*, Prentice-Hall, 1993.
- [13] Y. Li, L.J. Cimini Jr., N.R. Sollenberger, Robust channel estimation for OFDM systems with rapid dispersive fading channels, *IEEE Trans. Commun.* 46 (7) (1998) 902–915.
- [14] R.M. Mersereau, The processing of hexagonally sampled two dimensional signals, *Proc. IEEE* 67 (6) (1979) 930–949.
- [15] J.G. Proakis, *Digital Communications*, McGraw Hill, 2000.
- [16] T.F. Rappaport, *Wireless Communications: Principles and Practice*, second ed., Prentice-Hall, 2002.
- [17] P. Salvo Rossi, R.R. Müller, Joint iterative time-variant channel estimation and multi-user detection for MIMO-OFDM systems, in: *Proceedings of IEEE Global Telecommunications Conference (GLOBECOM)*, November 2007, pp. 1–6.
- [18] P. Salvo Rossi, R.R. Müller, Slepian-based two-dimensional estimation of time–frequency variant MIMO-OFDM channels, *IEEE Signal Process. Lett.* 15 (January) (2008) 21–24.
- [19] P. Salvo Rossi, R.R. Müller, Joint twofold-iterative channel estimation and multiuser detection for MIMO-OFDM systems, *IEEE Trans. Wireless Commun.* 7 (11) (2008) 4719–4729.
- [20] P. Salvo Rossi, R.R. Müller, O. Edfors, Slepian-based serial estimation of time–frequency variant channels for MIMO-OFDM systems, in: *Proceedings of IEEE Global Telecommunications Conference (GLOBECOM)*, December 2009, pp. 1–6.
- [21] N. Sarmadi, S. Shahbazpanahi, A.B. Gershman, Blind channel estimation in orthogonally coded MIMO-OFDM systems: a semidefinite relaxation approach, *IEEE Trans. Signal Process.* 57 (6) (2009) 2354–2364.
- [22] D. Slepian, Prolate spheroidal wave functions, Fourier analysis, and uncertainty—IV: extensions to many dimensions; generalized prolate spheroidal functions, *Bell Syst. Tech. J.* 43 (6) (1964) 3009–3058.
- [23] D. Slepian, Prolate spheroidal wave functions, Fourier analysis, and uncertainty—V: the discrete case, *Bell Syst. Tech. J.* 57 (5) (1978) 1371–1430.
- [24] G.L. Stüber, J.R. Barry, S.W. McLaughlin, Y. Li, M.A. Ingram, T.G. Pratt, Broadband MIMO-OFDM for wireless communications, *Proc. IEEE* 92 (2) (2004) 271–294.
- [25] L. Tong, B.M. Sadler, M. Dong, Pilot-assisted wireless transmissions: general model, design criteria, and signal processing, *IEEE Signal Process. Mag.* 21 (6) (2004) 12–25.
- [26] D. Tse, P. Viswanath, *Fundamentals of Wireless Communications*, Cambridge University Press, 2005.
- [27] D. Van De Ville, W. Phillips, I. Lemahieu, On the n -dimensional extension of the discrete prolate spheroidal window, *IEEE Signal Process. Lett.* 9 (3) (2002) 89–91.
- [28] X. Wang, H.V. Poor, Iterative (Turbo) soft interference cancellation and decoding for coded CDMA, *IEEE Trans. Commun.* 47 (7) (1999) 1046–1061.
- [29] B. Yang, K.B. Letaief, R.S. Cheng, Z. Cao, Channel estimation for OFDM transmission in multipath fading channels based on parametric channel modeling, *IEEE Trans. Commun.* 49 (3) (2001) 467–479.
- [30] S. Yatawatta, A.P. Petropulu, Blind channel estimation in MIMO OFDM systems with multiuser interference, *IEEE Trans. Signal Process.* 54 (3) (2006) 1054–1068.
- [31] T. Zemen, C.F. Mecklenbräuer, Time-variant channel estimation using discrete prolate spheroidal sequences, *IEEE Trans. Signal Process.* 53 (9) (2005) 3597–3607.
- [32] T. Zemen, C.F. Mecklenbräuer, J. Wehinger, R.R. Müller, Iterative joint time-variant channel estimation and multi-user detection for MC-CDMA, *IEEE Trans. Wireless Commun.* 5 (6) (2006) 1469–1478.
- [33] T. Zemen, H. Hofstetter, G. Steinböck, Successive slepian subspace projection in time and frequency for time-variant channel estimation, in: *Proceedings of IST Mobile and Wireless Communications Summit*, June 2005, pp. 1–5.
- [34] Y.R. Zheng, C. Xiao, Simulation models with correct statistical properties for Rayleigh fading channels, *IEEE Trans. Commun.* 51 (6) (2003) 920–928.